BJR

https://doi.org/10.1259/bjr.20190062

Received: 14 January 2019 | Revised: 26 March 2019 | Accepted: 23 April 2019

Cite this article as:
Kartamihardja AAP, Hanaoka H, Andriana P, Kameo S, Takahashi A, Koyama H, et al. Quantitative analysis of Gd in the protein content of the brain following single injection of gadolinium-based contrast agents (GBCAs) by size exclusion chromatography. *Br J Radiol* 2019; **92**: 20190062.

FULL PAPER

Quantitative analysis of Gd in the protein content of the brain following single injection of gadolinium-based contrast agents (GBCAs) by size exclusion chromatography

[1]ACHMAD ADHIPATRIA PERAYABANGSA KARTAMIHARDJA, MD, PhD, [2]HIROFUMI HANAOKA, PhD, [1]PUTRI ANDRIANA, MSc, [3]SATOMI KAMEO, PhD, [1]AYAKO TAKAHASHI, MD, PhD, [3]HIROSHI KOYAMA, MD, PhD and [1]YOSHITO TSUSHIMA, MD, PhD

[1]Department of Diagnostic Radiology and Nuclear Medicine, Gunma University Graduate School of Medicine, Japan
[2]Department of Bioimaging and Information Analysis, Gunma University Graduate School of Medicine, Japan
[3]Department of Public Health, Gunma University Graduate School of Medicine, Japan

Address correspondence to: Professor Yoshito Tsushima
E-mail: *yoshitotsushima@gunma-u.ac.jp*

Objective: To investigate the role of transporter proteins in gadolinium (Gd) distribution and retention in the brain after one high-dose injection of Gd-based contrast agent (GBCA).

Methods and materials: 30 ddY mice were randomly divided into three treatment groups to be intravenously injected with either Gadodiamide (linear GBCA), Gadobutrol (macrocyclic GBCA), or Gadoterate (macrocyclic GBCA) at a dose of 5 mmol/kg, while five mice in the control group received 250 µL saline. Five minutes (5 min) and ten days (10d) post-injection, the cerebrospinal fluid (CSF), choroid plexus (CP), and meninges and associated vasculature (MAV) were collected. The brain was then dissected to obtain the olfactory bulb, cerebral cortex, hippocampus, cerebellum, and brainstem. Proteins were extracted and separated by a size-exclusion high-performance liquid chromatography (SEC) system, and Gd concentrations were quantified by inductively coupled plasma mass spectrometry (ICP-MS).

Results: 5 m post-injection, the Gadodiamide group had the highest Gd concentration, while Gadoterate had the lowest Gd concentration in all parts of the brain ($p < .05$). Gd concentration was highest in the cerebrospinal fluid (CSF) of the Gadodiamide group (578.4 ± 135.3 nmol), while Gd concentration was highest in MAV in the Gadobutrol group (379.7 ± 75.4 nmol) at 5 min post-injection. At 10d, in spite of the significant decrease of Gd from all GBCAs ($p < 0.01$), retained Gd from Gadodiamide was detected all over the brain in several molecules that varied in size. Gd from Gadobutrol detected in the olfactory bulb (8.7 ± 4.5 nmol) was significantly higher than in other parts of the brain. Although most Gd from Gadobutrol was found in molecules similar in size to Gadobutrol, it was also found in several protein molecules of molecular size larger than the contrast agents. Only a small amount of Gd from Gadoterate was found in the brain.

Conclusion: GBCAs may be able to pass through intact brain barriers, and the chemical structures of GBCAs may affect the penetration capability of Gd into the brain. Retained Gd in the brain tissue from Gadodiamide and Gadobutrol may be bound to some organic molecules, including proteins.

Advances in knowledge: Intact GBCA are able to penetrate a series of brain barrier immediately after administration regardless the type of the chelate. Gd may be bound with macromolecules that may cause Gd retention in the brain.

INTRODUCTION

The paramagnetic properties of gadolinium (Gd) improve the diagnostic yield of MRI. Chelation of Gd greatly reduces its toxicity and enables its rapid elimination from the body. However, recent findings of unwanted signal intensity increase, which has been suspected to be related to Gd retention in the brains of patients with normal renal function, have invited heated discussion, especially on the safety of Gd-based contrast agent (GBCA) applications in clinical practice.[1,2] An *in vitro* study showed that GBCAs may disrupt the action of thyroid hormone on thyroid receptors of cerebellar Purkinje cells.[3] An *in vivo* study showed that

in utero exposure to GBCAs may impair memory function and coordination of adult mice.[4] The clinical implications of these findings have yet to be confirmed.

Although several studies have provided evidence of Gd retention in the brain,[5–9] the pathway of Gd penetration into the brain has yet to be elucidated. In order for Gd to be distributed into the brain, it must pass through a series of barriers that prevent the uptake of most substances: the blood-brain barrier (BBB), the circumventricular organs (CVO), and the blood-cerebrospinal fluid (CSF) barrier (choroid plexus).[10] These brain barrier systems protect the brain from harmful substances and regulate brain homeostasis.[10,11] They may also prevent uptake of heavy metals by the brain,[12] including intravenously administered GBCAs.

Stability and dissociation rates have been generally accepted to be crucial factors of Gd retention. Compared to macrocyclic GBCAs, the thermodynamic and kinetic parameters of linear GBCAs are less stable with higher dissociation rates.[13] Released Gd may bind to organic molecules, leading to Gd retention in the organs.[14,15] Gd is a heavy metal with an ionic radius similar to calcium,[16,17] so it might penetrate brain barriers through the activity of Ca^{2+} binding proteins or metal transporters. There is evidence that some commercially available GBCAs possess weak binding properties to proteins,[18,19] suggesting the possibility of endogenous proteins such as transferrin or albumin playing a role in Gd distribution into the brain. In addition, it has been reported that GBCAs potentially enter the brain by penetrating the choroid plexus, regardless of the chelate structure type.[20] Chromatographic methods such as size exclusion chromatography (SEC) can separate molecules based on their size, including large molecules such as proteins that may bind with Gd.

In this bioanalytic study, we investigated potential Gd-binding proteins in brain tissue by size-exclusion high-performance liquid chromatography (SEC).

METHODS AND MATERIALS

The institutional animal care and use committee of our institution approved all procedures in this study. 35 ddY mice (6 weeks old; mean weight 28.8 ± 0.8 g) were randomly divided into three treatment groups (n = 10 per group) to be intravenously injected with one injection (5 mmol/kg) of either Gadopentetate (Magnevist, 0.5 mol l^{-1}; Bayer Yakuhin Ltd., Osaka, Japan), Gadobutrol (Gadovist, 1 mol l^{-1}; Bayer Yakuhin Ltd., Osaka, Japan) or Gadoterate (Magnescope, 0.5 mol l^{-1}; Fuji Pharma, Toyama, Japan). Saline (5 mL/kg) was intravenously administered to five mice in the control group. All mice were housed in an approved animal facility with ad libitum access to food and water. Mice injected with different types of GBCAs were housed separately, and the author was blinded to the GBCA injected when the sample collection was done.

Injection and sampling protocol

The brain was collected either 5 min (n = 5/group) or 10d (n = 5/group) after the GBCA injection. Before we euthanized the mice, CSF was collected by the method established by Liu et al with slight modifications.[21] In brief, the mice were anesthetized by 3% isoflurane and the nape skin was shaved. Then, the mouse was placed prone on the stereotaxic equipment above a heating pad. When the head was secured, the surgical site was swabbed clean with 70% ethanol, and a 2 cm sagittal incision was made. Under a dissection microscope, the subcutaneous tissue and muscle were separated with forceps. After the mouse head was positioned at an approximately 135° angle with the body, the dura mater of the cisterna magna was exposed. The tapered tip of a glass capillary tube was inserted to the cisterna magna through the dura mater, lateral to the dorsal spinal artery. Roughly 10 µL of CSF was carefully collected from each mouse. The absence of blood contamination was observed visually.

Transcardial perfusion using phosphate buffer solution (PBS) was performed after CSF collection to remove excess blood from the brain. The mouse was euthanized by cervical dislocation under anesthesia. The brain was obtained and kept in ice-cold Hanks' balanced salt solution (HBSS) for 5 min. Subsequently, the choroid plexus (CP) and the meninges and associated vasculature (MAV) were carefully collected by the method described by Bowyer et al.[22] Then, the brain was dissected under a dissecting microscope, and samples from the olfactory bulb, cerebral cortex, hippocampus, cerebellum and brainstem were collected (Figure 1). Tissue protein extraction reagent (T-PER™; Thermo Scientific Inc., Japan) was added to the samples at a ratio of 1:10. After homogenization, the samples were subjected to centrifugation at 4°C and 10.000g for 5 min. The soluble fraction

Figure 1. Schematic diagram of dissected mouse brain showing olfactory bulb, cerebral cortex, hippocampus, cerebellum, brainstem, choroid plexus and MAV.

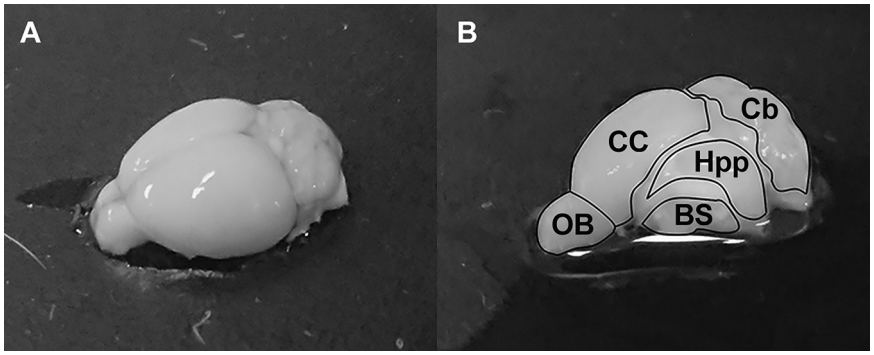

of the sample was collected and filtered by a 0.22 µm filter for molecular separation analysis.

Molecular separation method by SEC system

A high-performance SEC system (Waters Corp., Milford, MA), consisting of the Waters 600 controller, Waters 600 pump, and Waters 2487 Dual λ Absorbance Detector equipped with a TOSOH size-exclusion column (TSK gel superSW3000; column size: 4.6 mm I.D. x 30 cm; particle size: 4 µm, Tosoh, Tokyo, Japan) was used to separate the analytes based on their molecular size. The mobile phase was an aqueous buffer containing 100 mM ammonium acetate at a pH of 6.8, and the flow rate was 0.35 mL/min. After 100 µL of sample was injected, 20 fractions with a run time of 1 min/fraction were collected for mass spectrometry analysis. Transferrin, albumin and 10 µM of each respective contrast agent were used as standards to predict the molecular size distribution as interpreted on the chromatogram. The analytes with larger molecular size are separated earlier by the SEC machine, thus transferrin (80 kDa) and albumin (63 kDa) will elute faster than the GBCAs. The molecular weights of Gadopentetate, Gadobutrol and Gadoterate are 0.93 kDa, 0.6 kDa and 0.75 kDa, respectively.

Inductively coupled plasma mass spectrometry (ICP-MS) analysis for Gd concentration

The sample fractions collected from SEC underwent wet digestion with 100 µL of HNO_3 and 50 µL of H_2O_2 for 1 h. Then, 1.5 ml ultra-purified water was added to each sample. ^{158}Gd in each sample was measured by ICP-MS system ELAN® DRC II (PerkinElmer Inc., Waltham, MA). Verification of the ICP-MS system was performed using a linear regression graph of different concentrations of a standard Gd solution. Quantification of the ICP-MS analysis were verified in concentrations of up to 1.5 µmol (R = 0.99). The limit of detection (LoD; 0.04 nmol) and limit of quantification (LoQ; 0.19 nmol) of Gd concentration were determined based on pulse intensity of 15 nmol Gd standard solution.

Data analysis

All data were presented as mean and standard deviation (SD). The average Gd concentrations of each group were assessed using analysis of variance, followed by post-hoc Tukey's honest significant difference (HSD) test. SPSS software (version 24; IBM-SPSS, Inc., Chicago, IL) was used for data analyses. A p value of < 0.05 was considered to be statistically significant.

RESULTS

Gd concentration and the protein separation at 5min post-injection

The Gadopentetate group had the highest Gd concentration of the three GBCA groups ($p < .05$) in all parts of the brain. The highest Gd concentration from Gadopentetate was detected in the CSF (578.4 + 135.3 nmol) followed by MAV (570.8 + 183.7 nmol) and CP (179.9 + 49.4 nmol). Of the brain tissues, the highest Gd concentration was found in the cerebellum (143.1 + 49.9 nmol), followed by the olfactory bulb (104.1 + 20.2 nmol). The highest concentrations of Gd were found in molecules similar in size to Gadopentetate (0.93 kDa; Figure 2a).

In the Gadobutrol group, the highest Gd concentration was found in the MAV (379.7 + 75.4 nmol). The concentrations of Gd accumulated in the CSF and CP were 286.1 + 58.0 nmol and 83.9 + 19.9 nmol, respectively. The Gd concentrations among the remaining dissected brain parts were similar (p = .28, Table 1). The detected molecules with highest Gd concentration were consistent with the size of Gadobutrol (0.6 kDa; Figure 2b).

The Gadoterate group had the lowest average Gd concentration compared to the other treated groups ($p < .01$) in all samples. Gd from Gadoterate was detected at the highest concentration in CSF (204.8 + 40.9 nmol) of the areas examined. Gd found in the CP (27.9 + 11.1 nmol) and the MAV (57.0 + 14.4 nmol) of the Gadoterate group was significantly lower than that in the Gadopentetate and Gadobutrol groups ($p < .01$). Gd concentration was highest in the olfactory bulb (45.9 + 12.0 nmol),

Figure 2. Total Gd concentration in the mouse brain based on protein molecular size at 5 min after Gadopentetate (a), Gadobutrol(b) or Gadoterate(c) injection. Gadopentetate has the highest Gd concentration, while Gadoterate has the lowest concentration. The lines show the average pulse intensity on ICP-MS, while the symbol represents the total concentration of Gd (nmol).

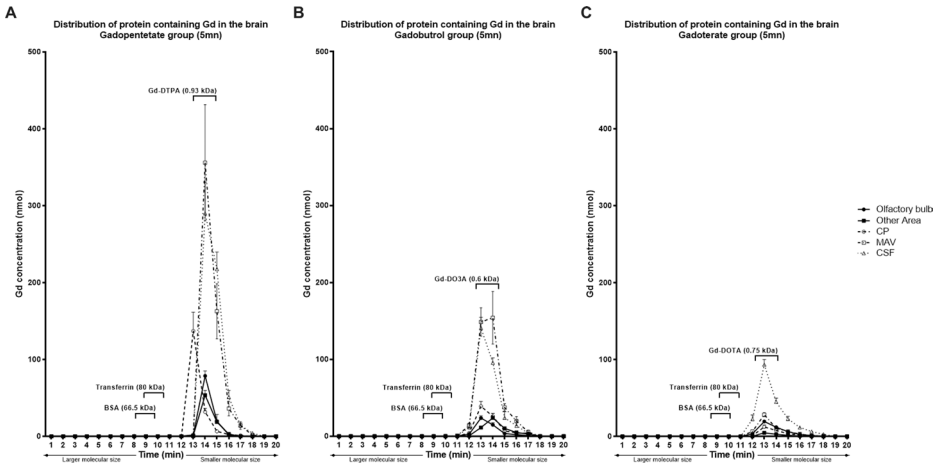

Table 1. Gd concentration in the brain of the mouse at 5 min and 10d after the injection of GBCAs, analyzed by ICP-MS

	Control	Gadopentetate (nmol)	Gadobutrol (nmol)	Gadoterate (nmol)	Gadopentetate (nmol)	Gadobutrol (nmol)	Gadoterate (nmol)
Olfactory bulb	[b]	104.1 ± 20.2[c]	47.9 ± 12.3	45.9 ± 12.0	8.3 ± 2.8	8.7 ± 4.5	[b]
Cerebral cortex	[b]	52.8 ± 16.9	60.9 ± 6.2	14.5 ± 6.0[d]	11.8 ± 7.0[c]	3.4 ± 1.2	[b]
Hippocampus	[b]	51.7 ± 14.6	40.5 ± 13.5	8.3 ± 2.5[d]	7.9 ± 1.3[c]	3.4 ± 1.6	[bd]
Cerebellum	[b]	143.1 ± 49.9[c]	58.3 ± 24.6	10.9 ± 5.5[d]	8.9 ± 3.5[c]	4.2 ± 3.3	0.5 ± 0.2
Brainstem	[b]	89.6 ± 24.1[c]	55.6 ± 17.7	10.0 ± 3.7[d]	9.0 ± 6.2[c]	2.3 ± 0.7	0.6 ± 0.4
CP	[b]	179.9 ± 49.4[c]	83.9 ± 19.9	27.9 ± 11.1[d]	22.6 ± 13.9	38.6 ± 8.2[c]	2.1 ± 1.6[d]
MAV	[b]	570.8 ± 183.7	379.7 ± 75.4	57.0 ± 14.4[d]	14.1 ± 8.0	30.9 ± 14.8[c]	1.4 ± 0.2
CSF	[b]	578.4 ± 135.3[c]	286.1 ± 58.0	204.8 ± 40.9	5.7 ± 2.2	3.9 ± 2.3	[b]

CP: Choroid plexus; CSF: Cerebrospinal fluid; MAV: Meningeal artery and vasculature.
All data are expressed by mean ± SD. *p* value of Gadopentetate, Gadobutrol and Gadoterate group at 5 min compared to the 10d group of the respective agent were <.01.
[a]ANOVA *p* value among GBCAs group was <.01
[b]Lower than the limit of quantification
[c]Significantly higher than the other GBCAs
[d]Significantly lower than the other GBCAs

compared to the other parts of the brain. In all areas of the brain, the highest Gd concentrations were observed at minute 13, which was consistent with the molecular size of Gadoterate (0.75 kDa; Figure 2c).

Gd concentration and protein separation at 10d post-injection

Ten days post-injection, Gd concentrations in the Gadopentetate and Gadobutrol groups were above the LoQ, while the average Gd concentration in the Gadoterate group was barely detected in the brain tissue. Gd in the CSF of all three GBCA treated groups was also barely detected.

Gd concentrations of the Gadopentetate group in each part of the dissected brain were significantly decreased compared to 5 min post-injection ($p < .01$), although small amounts of Gd were detected in the columns of molecular sizes larger than Gadopentetate (0.93 kDa), and small amounts were similar in size to albumin and transferrin (Figure 3a).

Similar results were also found in the Gadobutrol group. In brain tissue, the concentration of Gd retained in the Gadobutrol group was lower than that in the Gadopentetate group ($p < .01$) in all parts. However, it was higher in CP compared to other GBCAs ($p < .01$). In the Gadobutrol group, the olfactory bulb (8.7 + 4.5 nmol) had a significantly higher concentration of Gd compared to the other parts (3.4 + 1.9 nmol; $p = .03$). Although small amounts Gd from Gadobutrol was found in molecules with a size similar to Gadobutrol, it was also found in several molecules with molecular sizes larger than contrast agents (>0.6 kDa; Figure 3b). Meanwhile, a small amount of Gd from Gadoterate was detected in molecules with a size similar with intact Gadoterate.

Figure 3. Total Gd concentration in the mouse brain based on protein molecular size at 10d after Gadopentetate (a), Gadobutrol(b) or Gadoterate(c) injection. At 10d, there is a significant reduction of Gd concentration compared to the concentration at 5 min. Almost all Gd from Gadoterate was eliminated, while some Gd from Gadopentetate and Gadobutrol was retained throughout the brain.

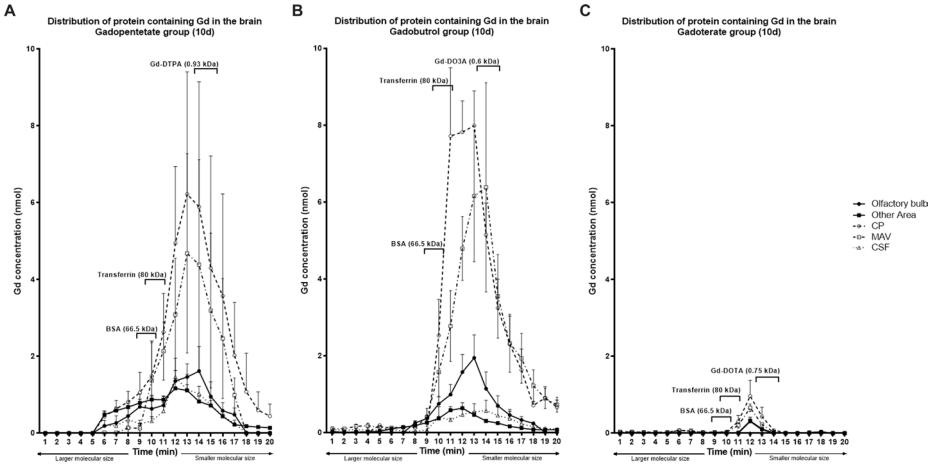

Figure 4. Proposed mechanism of GBCAs distribution into the brain via choroid plexus at 5 min. (a) Gd may bind with macromolecules and be distributed into the brain with the CSF, and may separates during its distribution into the brain. (b) Gd forms a weak bond with protein transporter in the circulation and enters the choroid plexus. Within the epithelial cells, these molecules separate from Gd and returns to the circulation, while Gd is secreted with CSF. (c) GBCAs may enter the brain via metal transporter or ion channel located on the choroid plexus membrane and secreted with CSF. (d) Delayed elimination of GBCA may cause Gd to separate from the chelate and bind with endogenous molecules,resulting in the formation of soluble complex and/or insoluble precipitation. The soluble complex may be eliminated faster through the glymphatic system, while the insoluble precipitation may be retained longer in the brain tissue.

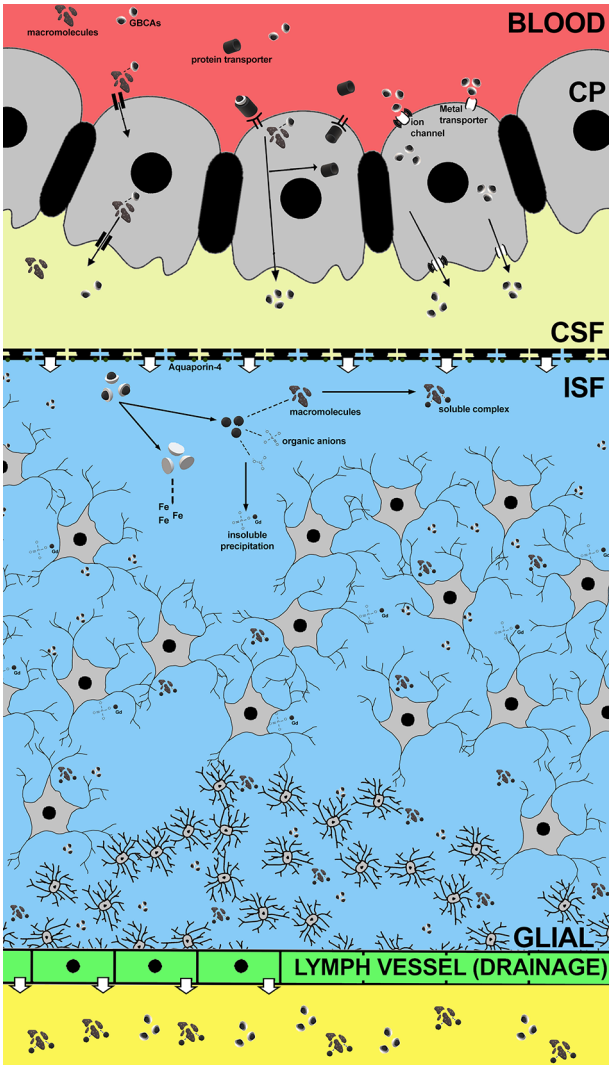

DISCUSSION

All GBCAs used in this study passed through the brain barrier within 5 min post-injection, regardless of the type of chelate. After 10d, several endogenous molecules were bound to Gd from Gadopentetate and Gadobutrol, while Gd from Gadoterate was found only in the molecules with a size similar with chelated form.

The total amount of Gd penetrating the brain barrier after 5 min varied among the three GBCAs. Gadopentetate had the highest penetration through the brain barrier, while Gadoterate had the lowest. These differences in Gd concentrations distributed in to the brain suggest that the chemical structures of GBCAs may play an important role in Gd distribution into the brain. In addition, the highest amount of Gd was detected in a fraction similar to that of GBCAs at 5 min, and Gd is unlikely to dissociate from GBCAs in such a short time. These results suggest that Gd may be able to penetrate the brain barrier and be distributed throughout the brain tissue in chelated form. Since it may be difficult for GBCAs to penetrate the brain barrier by themselves, some penetration mechanism may be required. We suspect that GBCAs may bind with some transporters in the blood, and that these mediate the transport of GBCA via the choroid plexus. The binding of GBCAs with the transporter may be weak and these complexes may be dissociated during analysing process. This would explain why the SEC only detected small molecules. The GBCAs in the CSF might then be distributed throughout the brain, with some penetrating deeply into the brain. Since the process of brain penetration of molecules is very slow,[23] the Gd observed in this study 5 min post-injection might be located in the extracellular space of the brain, while the Gd retained in the tissue at 10d may be located deep in the brain tissue.

In order for drugs, including GBCAs to enter the brain, they must penetrate the protective blood-brain barrier (BBB), circumventricular organs (CVO), and blood-cerebrospinal fluid barrier (choroid plexus).[24] The tight junctions of the BBB endothelial cells lack permeability and inhibit the free diffusion of water-soluble molecules.[25] Post-contrast MRI scans show no enhancement in the intra parenchymal portion of the BBB, suggesting that Gd cannot penetrate the brain via the BBB.[26] Although the CVO consists of extensive vasculature and fenestrated capillaries of the blood vessels,[27] its surface area is much smaller than the BBB,[26,28] suggesting that the CVO may not have significant involvement in Gd distribution into the brain.

On the other hand, the choroid plexus allows transport of select substances into the CSF, including drugs.[25] The choroid plexus actively secrets the CSF into the ventricles, and is the source of 80% CSF in the brain circulation.[29] We suspect that GBCAs may be able to pass through this selective barrier since high concentration of Gd in the CSF was found at 5 min post-injection. Taoka et. al. described the transition of gadopentetate from blood to CSF in no time as depicted by dynamic MRI, thus supporting our hypothesis that GBCAs are likely to be distributed via the choroid plexus.[30] Our result is also in accordance with Jost et. al., who state that considerable amount of GBCA was found in the CSF at 4 h after the injection of contrast agents.[20]

Conventional GBCAs have very little to no protein binding capability. We investigated the possibility of Gd binding with transferrin *in vivo* using SEC. Transferrin can be distinguished easily on the chromatogram, yet at 5 min post-injection we found no

significant traces of interaction between GBCAs and transferrin. There are two binding sites in transferrin that may interact with Gd enabling its distribution through the choroid plexus. Given the fact that the binding affinity of Gd to its chelates is at least 10^9-fold higher than that to transferrin,[31] it is unlikely that transmetalation occurs in the presence of transferrin. Meanwhile, albumin possesses specific sites for binding metal ions as well as calcium. Human serum albumin (HSA) has four sites that can bind with ligands, and a specific site for metal ions.[31,32] While albumin cannot pass through the BBB under normal conditions, it has been reported that it can pass through the choroid plexus.[33–35] Although it is possible that GBCAs interact with albumin and its binding proteins that were expressed in choroid plexus epithelial cells, the binding properties are likely very low. We also found no significant levels of albumin bound with GBCAs at 5 min post-injection. Considering one of the functions of the choroid plexus functions is preventing heavy metals from entering the brain, GBCAs may be transported into the brain through certain pathways, such as through channels, pumps or co-transporters, rather than just a simple filtration.

GBCAs dose in this study were equal to 0.4 mmol/Kg in humans[36] and were especially selected to observed the Gd-bound molecules at 10d after a single injection. At 10d, there was a small amount of Gd observed in multiple forms in the Gadopentetate and Gadobutrol groups. Proteins compose 10–13% of the brain content,[37] including protein transporters and neurotransmitter proteins. Calcium channels, another potential binding site for Gd, are also expressed in neurons[38]This may explain the low concentration of proteins found at 10d containing Gd from Gadopentetate and Gadobutrol. Also, other macromolecules may be the target of Gd transmetalation and eventually retained longer in the brain tissue.

Higher Gd concentrations in the olfactory bulb indicated that the glymphatic system may be responsible for Gd elimination from the brain.[39] The glymphatic system is a functional waste system of perivascular tunnels in the central nervous system. After being secreted by the choroid plexus, CSF will mix with the interstitial fluid (ISF) in order to facilitate brain metabolism, including the removal of waste and metabolites. A study of the olfactory nerves revealed that CSF and large contrast molecules drained into the veins and/or lymph vessels outside the nerve.[40] Moreover, Illif et al successfully described the brain waste pathway by using a dynamic scan with contrast agents. They showed that after contrast injections through the cisterna magna, the CSF influx for CSF-ISF change was found in several areas, and the CSF-ISF (and injected contrast) eventually reached the olfactory bulb.[41]The neuroprotective function of the glymphatic system works at its highest during sleep, when the brain removes toxic wastes.[42] This elimination process was also observed in a previous study, showing that injection of gadopentetate during long anaesthesia may lead to lower concentration of Gd deposition in the tissue.[30] Since the chemical structure of GBCAs differ, especially between the linear and macrocyclic type, the distribution and elimination process of each GBCA through the glymphatic system may also differ.

Delayed elimination of GBCAs from the brain may affect GBCA's kinetic stability, causing Gd to be dissociated from the chelate, and lead to Gd retention. Previous study showed that linear GBCAs may interfere with iron homeostasis and significantly increased cellular iron uptake from transferrin-dependent pathway.[43] Free iron is known to be involved in transmetalation of GBCAs and in extent were implicated in the pathogenesis of NSF. Both clinical and animal studies have confirmed gadolinium retention in the brain, especially in areas with high concentrations of iron, including the dentate nucleus of the cerebellum.[5] These areas are specifically affected by neurodegenerative disorders related to metal accumulation. Thus, Gd retained in these areas may be a potential risk for negative effect to brain function.

The chemical forms observed in this study were exclusively contained in the soluble portions. At 10d after injection, large molecular size proteins extracted from the brain of the Gadopentetate injected mice contained a higher concentration of Gd and had a greater variation in size compared to the Gadobutrol and Gadoterate groups. In order to exhibit signal intensity increase at low concentrations, Gd must attach to large macromolecules with slow tumbling rates.[44] These macromolecules (attached to Gd) may be responsible for the persistent signal intensity increase on T_1-weighted images reported in previous studies.[2,45] This would partially explain the hyperintensity being washed out when the use of the contrast agents is stopped.[46] Higher concentrations of linear contrast agents in the brain may contribute to higher Gd retention, and this may partially explain the phenomenon of retention when linear contrast agents are used in clinical practice.

There were some limitations to this study. The sample was exclusively proteins that were contained in the soluble portion of the samples, and the speciation of the insoluble form is unknown. Although samples were separated by molecular size, determining exactly which protein or macromolecule was bound to Gd was not possible due to the large number of molecules found in the brain. Also, the exact species of Gd could not be determined.

CONCLUSION

In conclusion, intact GBCAs may penetrate the brain barrier to be distributed into the brain tissue, and the chemical structures of GBCAs may affect the penetration capability of Gd into the brain. After 10 days, Gd from gadopentetate and gadobutrol detected in the brain tissue was bound to several large macromolecules. Although exactly which molecules were bound to Gd has yet to be elucidated, this mechanism may play a role in Gd retention in the brain.

DISCLOSURE

"We have read the guideline of British Journal of Radiology and declare that we have no conflict of interests nor financial interest on this article."

REFERENCES

1. Kanda T, Ishii K, Kawaguchi H, Kitajima K, Takenaka D. High signal intensity in the dentate nucleus and globus pallidus on unenhanced T1-weighted MR images: relationship with increasing cumulative dose of a gadolinium-based contrast material. *Radiology* 2014; **270**: 834–41. doi: https://doi.org/10.1148/radiol.13131669
2. Errante Y, Cirimele V, Mallio CA, Di Lazzaro V, Zobel BB, Quattrocchi CC, et al. Progressive increase of T1 signal intensity of the dentate nucleus on unenhanced magnetic resonance images is associated with cumulative doses of intravenously administered gadodiamide in patients with normal renal function, suggesting dechelation. *Invest Radiol* 2014; **49**: 685–90. doi: https://doi.org/10.1097/RLI.0000000000000072
3. Ariyani W, Iwasaki T, Miyazaki W, Khongorzul E, Nakajima T, Kameo S, et al. Effects of gadolinium-based contrast agents on thyroid hormone receptor action and thyroid hormone-induced cerebellar Purkinje cell morphogenesis. *Front Endocrinol* 2016; **7**: 115. doi: https://doi.org/10.3389/fendo.2016.00115
4. Khairinisa MA, Takatsuru Y, Amano I, Erdene K, Nakajima T, Kameo S, et al. The effect of perinatal gadolinium-based contrast agents on adult mice behavior. *Invest Radiol* 2018; **53**: 110–8. doi: https://doi.org/10.1097/RLI.0000000000000417
5. McDonald RJ, McDonald JS, Kallmes DF, Jentoft ME, Murray DL, Thielen KR, et al. Intracranial gadolinium deposition after contrast-enhanced MR imaging. *Radiology* 2015; **275**: 772–82. doi: https://doi.org/10.1148/radiol.15150025
6. Kanda T, Oba H, Toyoda K, Kitajima K, Furui S, et al. Brain gadolinium deposition after administration of gadolinium-based contrast agents. *Jpn J Radiol* 2016; **34**: 3–9. doi: https://doi.org/10.1007/s11604-015-0503-5
7. Kartamihardja AAP, Nakajima T, Kameo S, Koyama H, Tsushima Y. Impact of impaired renal function on gadolinium retention after administration of gadolinium-based contrast agents in a mouse model. *Invest Radiol* 2016; **51**: 655–60. doi: https://doi.org/10.1097/RLI.0000000000000295
8. Kartamihardja AAP, Nakajima T, Kameo S, et al. Distribution and clearance of retained gadolinium in the brain : differences between linear and macrocyclic gadolinium based contrast agents in a mouse model. *Br. J. Radiol* 2016; **1066**89.
9. Erdene K, Nakajima T, Kameo S, Khairinisa MA, Lamid-Ochir O, Tumenjargal A, et al. Organ retention of gadolinium in mother and pup mice: effect of pregnancy and type of gadolinium-based contrast agents. *Jpn J Radiol* 2017; **35**: 568–73. doi: https://doi.org/10.1007/s11604-017-0667-2
10. Laterra J, Keep R, Betz LA.Siegel G, Agranoff B, Albers W, eds. *Basic Neurochemistry: Molecular, Cellular and Medical Aspects (Blood—Brain Barrier). 6th Editio*. Philadelphia: Lippincott-Raven; 1999.
11. Ballabh P, Braun A, Nedergaard M. The blood-brain barrier: an overview: structure, regulation, and clinical implications. *Neurobiol Dis* 2004; **16**: 1–13. doi: https://doi.org/10.1016/j.nbd.2003.12.016
12. Zheng W, Perry DF, Nelson DL, Aposhian HV. Choroid plexus protects cerebrospinal fluid against toxic metals. *Faseb J* 1991; **5**: 2188–93. doi: https://doi.org/10.1096/fasebj.5.8.1850706
13. Idée JM, Port M, Robic C, et al. Role of thermodynamic and kinetic parameters in gadolinium chelate stability. In: *Journal of Magnetic Resonance Imaging. Vol 30. Wiley-Blackwell* 2009; 1249–58.
14. Frenzel T, Lengsfeld P, Schirmer H, Hütter J, Weinmann H-J. Stability of gadolinium-based magnetic resonance imaging contrast agents in human serum at 37 degrees C. *Invest Radiol* 2008; **43**: 817–28. doi: https://doi.org/10.1097/RLI.0b013e3181852171
15. Bleavins K, Perone P, Naik M, Rehman M, Aslam MN, Dame MK, et al. Stimulation of fibroblast proliferation by insoluble gadolinium salts. *Biol Trace Elem Res* 2012; **145**: 257–67. doi: https://doi.org/10.1007/s12011-011-9176-9
16. Bourne GW, Trifaró JM. The gadolinium ion: a potent blocker of calcium channels and catecholamine release from cultured chromaffin cells. *Neuroscience* 1982; **7**: 1615–22. doi: https://doi.org/10.1016/0306-4522(82)90019-7
17. Roland CR, Naziruddin B, Mohanakumar T, Flye MW. Gadolinium blocks rat Kupffer cell calcium channels: relevance to calcium-dependent prostaglandin E2 synthesis and septic mortality. *Hepatology* 1999; **29**: 756–65. doi: https://doi.org/10.1002/hep.510290345
18. Wang Y, Spiller M, Caravan P. Evidence for weak protein binding of commercial extracellular gadolinium contrast agents. *Magn Reson Med* 2010; **63**: 609–16. doi: https://doi.org/10.1002/mrm.22214
19. Cavagna FM, Maggioni F, Castelli PM, Daprà M, Imperatori LG, Lorusso V, et al. Gadolinium chelates with weak binding to serum proteins. A new class of high-efficiency, general purpose contrast agents for magnetic resonance imaging. *Invest Radiol* 1997; **32**: 780–96.
20. Jost G, Frenzel T, Lohrke J, Lenhard DC, Naganawa S, Pietsch H, et al. Penetration and distribution of gadolinium-based contrast agents into the cerebrospinal fluid in healthy rats: a potential pathway of entry into the brain tissue. *Eur Radiol* 2017; **27**: 2877–85. doi: https://doi.org/10.1007/s00330-016-4654-2
21. Liu L, Duff K. A technique for serial collection of cerebrospinal fluid from the cisterna MagNA in mouse. *JoVE* 2008; **21**. doi: https://doi.org/10.3791/960
22. Bowyer JF, Thomas M, Patterson TA, et al. A visual description of the dissection of the cerebral surface vasculature and associated meninges and the choroid plexus from rat brain. *J. Vis. Exp* 2012; **69**: 1–7.
23. Spector R, Keep RF, Robert Snodgrass S, Smith QR, Johanson CE. A balanced view of choroid plexus structure and function: focus on adult humans. *Exp Neurol* 2015; **267**: 78–86. doi: https://doi.org/10.1016/j.expneurol.2015.02.032
24. Daneman R, Prat A. The blood-brain barrier. *Cold Spring Harb Perspect Biol* 2015; **7**: a020412. doi: https://doi.org/10.1101/cshperspect.a020412
25. Rouault TA, Zhang D-L, Jeong SY. Brain iron homeostasis, the choroid plexus, and localization of iron transport proteins. *Metab Brain Dis* 2009; **24**: 673–84. doi: https://doi.org/10.1007/s11011-009-9169-y
26. Levy LM. Exceeding the limits of the normal blood-brain barrier: quo vadis gadolinium? *AJNR Am J Neuroradiol* 2007; **28**: 1835–6. doi: https://doi.org/10.3174/ajnr.A0725
27. Cottrell GT, Ferguson AV. Sensory circumventricular organs: central roles in integrated autonomic regulation. *Regul Pept* 2004; **117**: 11–23. doi: https://doi.org/10.1016/j.regpep.2003.09.004
28. Gross PM, Blasberg RG, Fenstermacher JD, Patlak CS. The microcirculation of rat circumventricular organs and pituitary gland. *Brain Res Bull* 1987; **18**: 73–85. doi: https://doi.org/10.1016/0361-9230(87)90035-9
29. Damkier HH, Brown PD, Praetorius J. Cerebrospinal fluid secretion by the choroid plexus. *Physiol Rev* 2013; **93**: 1847–92. doi: https://doi.org/10.1152/physrev.00004.2013

30. Taoka T, Jost G, Frenzel T, Naganawa S, Pietsch H. Impact of the Glymphatic system on the kinetic and distribution of gadodiamide in the rat brain: observations by dynamic MRI and effect of circadian rhythm on tissue gadolinium concentrations. *Invest Radiol* 2018; **53**: 529–34. doi: https://doi.org/10.1097/RLI.0000000000000473
31. Prybylski JP, Maxwell E, Coste Sanchez C, Jay M. Gadolinium deposition in the brain: lessons learned from other metals known to cross the blood-brain barrier. *Magn Reson Imaging* 2016; **34**: 1366–72. doi: https://doi.org/10.1016/j.mri.2016.08.018
32. Fasano M, Curry S, Terreno E, Galliano M, Fanali G, Narciso P, et al. The extraordinary ligand binding properties of human serum albumin. *IUBMB Life* 2005; **57**: 787–96. doi: https://doi.org/10.1080/15216540500404093
33. Liddelow SA. Development of the choroid plexus and blood-CSF barrier. *Front Neurosci* 2015; **9**(MAR): 1–13. doi: https://doi.org/10.3389/fnins.2015.00032
34. Liddelow SA, Dziegielewska KM, Møllgård K. Cellular specificity of the blood-CSF barrier for albumin transfer across the choroid plexus epithelium. Bisser S, ed. PLoS One. 2014;9(9).. Available from: http://dx.plos.org/10.1371/journal.pone.0106592 [Accessed February 14, 2018].
35. Knott GW, Dziegielewska KM, Habgood MD, Li ZS, Saunders NR. Albumin transfer across the choroid plexus of South American opossum (Monodelphis domestica. *J Physiol* 1997; **499 (Pt 1**: 179–94. doi: https://doi.org/10.1113/jphysiol.1997.sp021919
36. Nair A, Jacob S. A simple practice guide for dose conversion between animals and human. *J Basic Clin Pharm* 2016; **7**: 27–31. doi: https://doi.org/10.4103/0976-0105.177703
37. Banay-Schwartz M, Kenessey A, DeGuzman T, Lajtha A, Palkovits M, et al. Protein content of various regions of rat brain and adult and aging human brain. *AGE* 1992; **15**: 51–4. doi: https://doi.org/10.1007/BF02435024
38. Elmslie KS. Neurotransmitter modulation of neuronal calcium channels. *J Bioenerg Biomembr* 2003; **35**: 477–89. doi: https://doi.org/10.1023/B:JOBB.0000008021.55853.18
39. Rasschaert M, Schroeder JA, Wu T-D, Marco S, Emerit A, Siegmund H, Di WT, et al. Multimodal imaging study of gadolinium presence in rat cerebellum: differences between Gd chelates, presence in the Virchow-Robin space, association with lipofuscin, and hypotheses about distribution pathway. *Invest Radiol* 2018; **53**: 518–28. doi: https://doi.org/10.1097/RLI.0000000000000490
40. Jessen NA, Munk ASF, Lundgaard I, Nedergaard M, et al. The Glymphatic System: A Beginner's Guide. *Neurochem Res* 2015; **40**: 2583–99. doi: https://doi.org/10.1007/s11064-015-1581-6
41. Iliff JJ, Lee H, Yu M, Feng T, Logan J, Nedergaard M, et al. Brain-wide pathway for waste clearance captured by contrast-enhanced MRI. *J Clin Invest* 2013; **123**: 1299–309. doi: https://doi.org/10.1172/JCI67677
42. Eugene AR, Masiak J. The neuroprotective aspects of sleep. *MEDtube Sci* 2015; **3**: 35–40.
43. Swaminathan S. Gadolinium toxicity: iron and ferroportin as central targets. *Magn Reson Imaging* 2016; **34**: 1373–6. doi: https://doi.org/10.1016/j.mri.2016.08.016
44. Frenzel T, Apte C, Jost G, Schöckel L, Lohrke J, Pietsch H, et al. Quantification and assessment of the chemical form of residual gadolinium in the brain after repeated administration of gadolinium-based contrast agents: comparative study in rats. *Invest Radiol* 2017; **52**: 396–404. doi: https://doi.org/10.1097/RLI.0000000000000352
45. Jost G, Lenhard DC, Sieber MA, Lohrke J, Frenzel T, Pietsch H, et al. Signal increase on unenhanced T1-weighted images in the rat brain after repeated, extended doses of gadolinium-based contrast agents: comparison of linear and macrocyclic agents. *Invest Radiol* 2016; **51**: 83–9. doi: https://doi.org/10.1097/RLI.0000000000000242
46. Behzadi AH, Farooq Z, Zhao Y, Shih G, Prince MR. Dentate nucleus signal intensity decrease on T1-weighted MR images after switching from gadopentetate dimeglumine to Gadobutrol. *Radiology* 2018; **287**: 816–23. doi: https://doi.org/10.1148/radiol.2018171398